HHS Public Access

Author manuscript

Eur J Nucl Med Mol Imaging. Author manuscript; available in PMC 2018 August 01.

Published in final edited form as:

Eur J Nucl Med Mol Imaging. 2017 August ; 44(8): 1296–1305. doi:10.1007/s00259-017-3663-y.

Radiolabeled pertuzumab for imaging of human epidermal growth factor receptor 2 expression in ovarian cancer

Dawei Jiang[‡,1,2], **Hyung-Jun Im**[‡,2,3], **Haiyan Sun**[‡,2], **Hector F. Valdovinos**[4], **Christopher G. England**[4], **Emily B. Ehlerding**[4], **Robert J. Nickles**[4], **Dong Soo Lee**[3], **Steve Y. Cho**[2], **Peng Huang**[*,1], and **Weibo Cai**[*,2,4,5]

[1]Guangdong Key Laboratory for Biomedical Measurements and Ultrasound Imaging, School of Biomedical Engineering, Shenzhen University, Shenzhen, 518060, China

[2]Department of Radiology, University of Wisconsin - Madison, WI 53705, USA

[3]Department of Nuclear Medicine, Seoul National University, Seoul 110-744, Korea

[4]Department of Medical Physics, University of Wisconsin - Madison, Madison, WI 53705, USA

[5]University of Wisconsin Carbone Cancer Center, Madison, WI 53705, USA

Abstract

Purpose—Human epidermal growth factor receptor 2 (HER2) is overexpressed in over 30% of ovarian cancer cases, playing essential roles in tumorigenesis and metastasis. Non-invasive imaging of HER2 is of great interest for physicians to better detect and monitor the progression of ovarian cancer. In this study, HER2 was assessed as a biomarker for ovarian cancer imaging using ^{64}Cu-labeled pertuzumab for immunoPET imaging.

Methods—HER2 expression and binding were examined in three ovarian cancer cell lines (SKOV3, OVCAR3, Caov3) using *in vitro* techniques, including Western blot and saturation binding assays. PET imaging and biodistribution studies in subcutaneous models of ovarian cancer were performed to non-invasively evaluate HER2 expression *in vivo*. Additionally, orthotopic models were employed to further validate the imaging capability of ^{64}Cu-NOTA-pertuzumab.

Results—HER2 expression was highest in SKOV3 cells, while OVCAR3 and Caov3 displayed lower HER2 expression. ^{64}Cu-NOTA-pertuzumab showed high specificity to HER2 (K_a = 3.1 ± 0.6 nM) in SKOV3. In subcutaneous tumors, PET imaging revealed tumor uptakes of 41.8 ± 3.8, 10.5 ± 3.9, and 12.1 ± 2.3 %ID/g at 48 h post-injection for SKOV3, OVCAR3, and Caov3, respectively (n=3). In orthotopic models, PET imaging with ^{64}Cu-NOTA-pertuzumab allowed for rapid and clear delineation of both primary and small peritoneal metastases in HER2-overexpressing ovarian cancer.

[*]**Corresponding Author**: Weibo Cai, Ph.D. Room 7137, 1111 Highland Ave, Madison, WI 53705-2275, USA. wcai@uwhealth.org; Phone: 608-262-1749; Fax: 608-265-0614.

[‡]These authors contributed equally to this work

Conflict of Interest: The authors declare that they have no conflict of interest.

Ethical approval: All applicable international, national, and/or institutional guidelines for the care and use of animals were followed.

Conclusion—^{64}Cu-NOTA-pertuzumab is an effective PET tracer for the non-invasive imaging of HER2-expression *in vivo*, making it a potential tracer for treatment monitoring and improved patient stratification in the future.

Keywords

Positron emission tomography (PET); human epidermal growth factor receptor 2 (HER2); pertuzumab; ovarian cancer; molecular imaging

Introduction

Human epidermal growth factor receptor 2 (HER2) is a receptor overexpressed in 15–40% of patients with ovarian cancer and plays a major role in cell growth, proliferation, and differentiation [1–3]. In particular, HER2-directed therapy reduced tumor progression in a xenograft model of ovarian cancer [4]. Also, HER2-directed therapy is standard of care for HER2-positive breast cancer and under clinical evaluation in ovarian cancer [5, 6]. Currently, HER2 status is examined by fluorescence in situ hybridization or immunohistochemistry using tumor biopsy samples. However, the heterogeneous expression of HER2 within patients may lead to unpredictable biopsy results [7, 8]. Non-invasive imaging of HER2 expression can allow physicians to monitor HER2-directed therapies in patients, while also assisting in patient stratification.

Pertuzumab is an HER2-targeting monoclonal antibody, which was approved by the Food and Drug Administration after a clinical trial proved the survival benefit of pertuzumab in HER2-positive metastatic breast cancer [9]. Also, in combination with trastuzumab, pertuzumab showed enhanced antitumor effect in xenograft models of human ovarian cancer [10]. The potential of pertuzumab as an imaging probe for HER2-positive cancer has also been reported using fluorescently-labeled pertuzumab [11]. More importantly, pertuzumab can be utilized as an imaging tracer in patients who treated with trastuzumab, because trastuzumab and pertuzumab do not affect the binding of the other [12]. However, pertuzumab has not been well investigated as a tracer for positron emission tomography (PET) imaging which has higher sensitivity and quantification abilities than optical imaging.

In 2016, there will be an estimated 22,280 new cases of ovarian cancer, along with 14,240 attributed deaths [13]. This highly aggressive disease will result in 54% of patients succumbing to ovarian cancer within five years. The increased mortality attributed to ovarian malignancies is related to the fact that most patients (> 85%) are diagnosed during late disease stages with widely-spread metastatic tumors in the peritoneal cavity. Herein, we describe the development and evaluation of a ^{64}Cu-labeled PET tracer (^{64}Cu-NOTA-pertuzumab) for the *in vivo* imaging of HER2-positive ovarian cancer using pertuzumab. We hypothesized that PET imaging using ^{64}Cu-NOTA-pertuzumab could allow for *in vivo* evaluation of relative HER2 expression and sensitive detection of HER2-positive tumor in both subcutaneous and orthotopic models of ovarian cancer.

Materials and Methods

Cell culture

Human ovarian adenocarcinoma cell lines (SKOV3, OVCAR3, and Caov3) were purchased from American Type Culture Collection (Manassas, VA, USA) and cultured in Dulbecco's modified Eagle's medium (DMEM) supplemented with 10% fetal bovine serum (FBS; Hyclone, GE Healthcare, Little Chalfont, UK) at 37 °C in a humidified incubator with 5% CO_2.

Animal models

All animal operations were carried out under a protocol approved by the University of Wisconsin Institutional Animal Care and Use Committee. Subcutaneous tumors (SKOV3, OVCAR3, and Caov3) were engrafted into 4–6 weeks-old female athymic nude mice (Crl: NU(NCr)-Foxn1nu) obtained from Envigo (Indianapolis, IN, USA). For implantation, 2×10^6 cancer cells in 100 μL Matrigel (BD Biosciences, San Jose, CA, USA) were subcutaneously injected into the lower right flank of each mouse. For orthotopic implantation of SKOV3 and OVCAR3 tumors, mice were anesthetized with 2–4% isoflurane and placed dorsal side up. An incision was made to the right of the midline and above the ovaries. Next, 1×10^6 cancer cells in 10 μL of Matrigel were slowly injected into the ovaries before the incision was closed with absorbable 6–0 sutures (Ethicon, Cincinnati, OH, USA).

Western blot

For Western blot, cancer cells were harvested, and total protein concentration was measured with the Pierce Coomassie protein assay kit (ThermoFisher Scientific). Thirty μg of total protein was loaded into the wells of a 4–12% Bolt Bis-Tris Plus gel (ThermoFisher Scientific), along with the Chameleon Duo ladder (LI-COR Biosciences, Lincoln, NE, USA). After electrophoresis at 120 mV for 60 min at 4 °C, proteins were transferred to a nitrocellulose membrane using the iBlot 2 (ThermoFisher Scientific). Next, the membrane was blocked with Odyssey blocking buffer (LI-COR Biosciences) and incubated with 1:200 pertuzumab antibody and 1:200 β-actin antibody (Novus Biologicals, Littleton, CO, USA) for 12 h at 4 °C. Next, the membrane was washed three times with PBS-T (phosphate buffered saline with Tween 20) before secondary antibody incubation with goat anti-human DyLight 800 and donkey anti-mouse DyLight 680 (Novus Biologicals). The membrane was scanned using the LI-COR Odyssey infrared imaging system (LI-COR Biosciences).

Flow cytometry

Cells were suspended in cold phosphate buffered saline (PBS) with 2% bovine serum albumin (BSA) at the concentration of ~ 1×10^6 cells per mL. Cells were incubated with 200 μL of pertuzumab (25 μg/mL in PBS with 2% BSA) on ice for 30 min, and then washed with cold PBS three times. After re-suspending in cold PBS, cells were then incubated with fluorescence isothiocyanate (FITC)-labeled goat anti-human secondary antibody (Novus Biologicals) on ice for 30 min. The cells were analyzed using the MACSQuant cytometer (Miltenyi Biotec, Bergisch Gladbach, Germany) and mean fluorescence intensities were processed using the FlowJo software (Tree Star, Ashland, OR, USA).

NOTA conjugation and ^{64}Cu-labeling of pertuzumab

The detailed methods for 1,4,7-triazacyclononane-triacetic acid (NOTA) conjugation and ^{64}Cu labeling with antibodies have been previously reported [14, 15]. Briefly, pertuzumab was mixed with p-SCN-Bn-NOTA in dimethyl sulfoxide (DMSO) and incubated at pH 8.5–9.0 at room temperature for 2 h. NOTA-pertuzumab was purified using PD-10 desalting column with 1 × PBS as the elution buffer. ^{64}Cu was produced by a PETrace cyclotron (GE Healthcare) using the ^{64}Ni(p,n)^{64}Cu reaction. For the radiolabeling of NOTA-pertuzumab, ^{64}Cu (~37 MBq) was diluted with sodium acetate and mixed with NOTA-pertuzumab (~1 mg/mL). Following 1 h incubation at 37 °C with constant shaking, the mixed solution was purified using a PD-10 column. Human serum IgG was used as non-specific antibody and labeled with the same method to obtain ^{64}Cu-NOTA-IgG$_{Nonspecific}$.

Saturation binding assay

SKOV3 cells were seeded in a 96-well plate at 1 × 10^6 cells per well. ^{64}Cu-NOTA-pertuzumab solution was prepared in PBS (containing 0.1% BSA) with gradient concentration from 0.03–100 nM. After adding antibody solutions to each well, cells were incubated at room temperature for 2 h. To determine the non-specific binding of ^{64}Cu-NOTA-pertuzumab, 1 μmol of unlabeled pertuzumab was added. At the end of the 2 h incubation, cells were washed with PBS three times and harvested for gamma counter analysis. Based on the overall and nonspecific ligands bound to SKOV3 cells, the K_a and B_{max} values were determined, and the HER2 receptor density on SKOV3 cells was determined using GraphPad Prism software (La Jolla, CA, USA).

PET/CT imaging and biodistribution

PET imaging was performed on the Inveon micro-PET/CT rodent model scanner (Siemens Medical Solutions, Erlangen, Germany). Tumor-bearing mice were intravenously (i.v.) injected with 5–10 MBq of ^{64}Cu-NOTA-pertuzumab or ^{64}Cu-NOTA-IgG$_{Nonspecific}$, and PET scans were conducted at 3, 24, and 48 h after injection. For orthotopic groups, PET/CT scans were performed at the last time point. Following the terminal PET or PET/CT scan, mice were sacrificed, and organs of interest were harvested to validate the imaging data. A gamma counter (PerkinElmer, Waltham, MA, USA) was used to quantify tracer uptake in various tissues and organs, and accumulations were denoted by percentage of injected dose per gram of tissue (%ID/g; ≥ 3 mice per group).

Immunofluorescence staining

Tumors were extracted, and sectioning was performed by the University of Wisconsin Carbone Cancer Center Experimental Pathology Laboratory. Frozen tumor tissue slices of 5-mm thickness were fixed with cold acetone for 10 min, washed with PBS, and then blocked with 10% donkey serum for 45 min at room temperature. Slices were then incubated overnight with pertuzumab (10 μg/mL) and rat anti-mouse CD31 (2 μg/mL; ThermoFisher Scientific) at 4 °C. Next, sections were further stained with AlexaFluor488-labeled goat anti-human antibody and Cy3-labeled donkey anti-rat antibodies (ThermoFisher Scientific). A coverglass was applied to each slide using Vectashield mounting medium (Vector

Laboratories, Burlingame, CA, USA) and imaging was performed using an A1R confocal microscope (Nikon, Nikon Instruments, Melville, NY, USA).

Ultrasonography detection of orthotopic tumors

Ultrasound imaging (VisualSonics Vevo 2100, Toronto, Canada) was performed in mice weekly to monitor tumor development. 2D images of mouse ovaries were acquired using a linear-array transducer (MS-400) in B-mode with 30-MHz center frequency.

Dosimetry

Dosimetry analysis was performed using OLINDA/EXM software [16]. Estimated human dosimetry was calculated using %ID/g values from the serial PET scans on mice injected with ^{64}Cu-labeled pertuzumab. It was assumed that the biodistribution in adult humans was the same as in the animal models, and a triexponential model was utilized for the time-activity curves. OLINDA provides effective dose outputs; thus, weighting factors from ICRP 103 were employed to convert to absorbed dose in each organ [17].

Statistical analysis

Quantitative data were displayed as mean ± standard deviation (SD). Means were compared using the Student *t*-test and p-values < 0.05 were considered statistically significant.

RESULTS

HER2 expression in ovarian cancer cell lines

Relative expression levels of HER2 in three ovarian cancer cell lines were determined using Western blot with pertuzumab as the primary antibody. A 110-kDa band was seen in each lane representing HER2, while β-actin was visible at 38-kDa (Fig. 1a). SKOV3 cells showed the strongest band intensity at 110-kDa, indicating the highest expression of HER2, while OVCAR3 and Caov3 cells both displayed low levels of HER2 expression.

Cell binding affinity of pertuzumab to HER2

The binding affinity of pertuzumab with cellular HER2 was examined through flow cytometry studies. A significant shift along the x-axis denoted strong binding of pertuzumab to the cell line. A strong fluorescent signal shift was shown in the SKOV3 group, indicating enhanced binding of pertuzumab to SKOV3 (Fig. 1b). The shifts for OVCAR3 and Caov3 groups were smaller than that of the SKOV3 group, suggesting lower binding of HER2.

Saturation binding assay with ^{64}Cu-NOTA-pertuzumab for SKOV3 cells

A saturation binding assay was performed to quantify the maximum binding and HER2-affinity constant (K_a) of ^{64}Cu-NOTA-pertuzumab with SKOV3 cells. Rapid saturation of HER2 was achieved using 30 nM ^{64}Cu-NOTA-pertuzumab, and the K_a value was calculated to be 3.1 ± 0.6 nM (Fig. 1c). The receptor density in SKOV3 was determined to be (1.63 ± 0.12) × 10^6 HER2 receptors per cell.

ImmunoPET imaging and biodistribution of ^{64}Cu-NOTA-pertuzumab in subcutaneous tumors

Serial PET scans were completed with ^{64}Cu-NOTA-pertuzumab at 3, 24, and 48 h after injection of the tracer. Maximum intensity projections (MIPs) of PET images are shown in Fig. 2a. The quantitative data were obtained from the region-or-interest (ROI) analyses and shown in Fig. 2b. At all imaging time points, the SKOV3 group showed the highest tumor accumulation among three study groups, with 16.8 ± 3.9, 38.6 ± 6.7, and 41.8 ± 3.8 %ID/g at 3, 24, and 48 h after injection, respectively (n=3). Tumor accumulations of both OVCAR3 and Caov3 groups were significantly lower than that of SKOV3 group, with the highest tumor accumulation of 13.6 ± 4.7 %ID/g for the OVCAR3 model and 10.2 ± 4.5 %ID/g for the Caov3 model at 48 h after injection (n=3; $p<0.01$ at each time point).

To ensure the uptake of ^{64}Cu-NOTA-pertuzumab was specific, a nonspecific antibody (^{64}Cu-NOTA-IgG$_{Nonspecific}$) was injected to SKOV3 tumor-bearing mice (Fig. S1). While blood uptake of both tracers was comparable at each time point, the tumor uptake of ^{64}Cu-NOTA-IgG$_{Nonspecific}$ was significantly lower than that of ^{64}Cu-NOTA-pertuzumab with uptake values of 7.2 ± 1.6 and 41.8 ± 3.8 %ID/g at 48 h after injection (n=4, $p<0.01$), respectively; thus, confirming the *in vivo* binding specificity of ^{64}Cu-NOTA-pertuzumab for HER2-expressing tumors (Fig. S1).

Biodistribution studies were performed to validate PET analyses. The *ex vivo* biodistribution of ^{64}Cu-NOTA-pertuzumab in SKOV3 tumors was 42.3 ± 10.3 %ID/g, significantly higher than those of OVCAR3 and Caov3 tumors with activity values of 10.5 ± 3.9 and 12.1 ± 2.3 %ID/g, respectively (Fig. S2; $p<0.05$, n=3). Tracer uptake in other organs, including the liver, spleen, lung, and kidneys, were similar among the models. Also, ^{64}Cu-NOTA-IgG$_{Nonspecific}$ exhibited minimal tumor accumulation with activity values of 5.0 ± 0.5 %ID/g at 48 h after injection (Fig. S3, n=4; $p<0.01$). Overall, the *ex vivo* biodistribution study confirmed the excellent *in vivo* HER2-targeting ability of ^{64}Cu-NOTA-pertuzumab.

Immunofluorescence co-staining of HER2 and CD31

SKOV3 tumor sections showed the highest expression of HER2, while tumor sections from OVCAR3 and Caov3 groups displayed lower levels (Fig. 3). The HER2 staining intensities correlated well with tumor uptakes in all three groups, further solidifying the ability of ^{64}Cu-NOTA-pertuzumab PET to assess HER2 expression noninvasively in ovarian cancer.

ImmunoPET imaging and biodistribution of ^{64}Cu-NOTA-pertuzumab in orthotopic tumors

The presence of ovarian tumors was verified using ultrasonography (Fig. S4). Primary tumors could be clearly identified in both SKOV3 and OVCAR3 orthotopic models of ovarian cancer using PET/CT imaging (Fig. 4). SKOV3 orthotopic tumors showed enhanced accumulation of ^{64}Cu-NOTA-pertuzumab that increased from 11.4 ± 2.8 %ID/g to 29.8 ± 13.3 %ID/g at 3 h and 48 h after injection, respectively; whereas, OVCAR3 orthotopic tumors showed persistent, yet low tumor uptake of 8–9 %ID/g at all time points (Fig. S5).

The primary tumors and peritoneal metastases were visually verified through autopsy. Primary tumors could be easily delineated from PET/CT imaging in both orthotopic tumor

models (Fig. 5). In the images, additional focal uptakes were found in the peritoneal space of the SKOV3 group suspected to be peritoneal implants (Fig. 5a). The white nodular tissues with high tracer uptake were extracted for further evaluation (Fig. 5b). The tissues were confirmed to be HER2-positive peritoneal implants by *ex vivo* PET imaging. Five peritoneal implants sized from 2–5 mm were discovered in three SKOV3 mice with high uptake from 14.4 to 18.6 %ID/g (Fig. 5c). Peritoneal implants were not found in the OVCAR3 orthotopic tumor model, suggesting that PET imaging using ^{64}Cu-NOTA-pertuzumab may allow for sensitive detection of small peritoneal implants in HER2-positive ovarian cancer.

Ex vivo biodistribution studies showed 23.3 ± 4.8 %ID/g tumor uptake in the SKOV3 group, which was significantly higher than that of the OVCAR3 group with a tumor uptake of 8.7 ± 3.0 %ID/g (n=3, $p<0.05$). Normal ovaries showed tracer uptakes of 4.08 ± 1.6 %ID/g and 4.5 ± 0.6 %ID/g for SKOV3 and OVCAR3 models, respectively (Fig. 6). Overall, imaging with ^{64}Cu-NOTA-pertuzumab enabled non-invasive assessment of HER2 expression.

Radiation dosimetry of ^{64}Cu-NOTA-pertuzumab

Human absorbed doses to normal organs were estimated based on the biodistribution of ^{64}Cu-NOTA-pertuzumab (n=4) and organs with high absorbed doses were the liver ($1.2 \pm 0.1 \times 10^{-1}$ mSv/MBq), ovary ($6.6 \pm 0.4 \times 10^{-2}$ mSv/MBq), heart wall ($3.9 \pm 0.2 \times 10^{-2}$ mSv/MBq), and lung ($4.3 \pm 0.7 \times 10^{-2}$ mSv/MBq), as shown in Table S1. The total whole-body effective dose was $(2.9 \pm 0.1) \times 10^{-2}$ mSv/MBq, which was far lower than previously determined using ^{89}Zr-labeled antibodies [18, 19].

Discussion

In the present study, ^{64}Cu-NOTA-pertuzumab was developed and investigated for HER2-targeted imaging of ovarian cancer. Three ovarian cancer cell lines were selected and confirmed to have different levels of relative HER2 expression (SKOV3: high, OVCAR3: low, Caov3: low). All tumors from three subcutaneous models were clearly visualized with SKOV3 tumors showing nearly 42 %ID/g, about four-times higher than that of OVCAR3 and Caov3 groups, and eight-times higher than nonspecific IgG. Also, the specific HER2-targeting ability of ^{64}Cu-NOTA-pertuzumab enabled sensitive and specific tumor detection in the orthotopic models of ovarian cancer. We could readily recognize the location of the primary tumors in SKOV3 and OVCAR3 orthotopic models and small peritoneal implants (2–5 mm) in SKOV3 tumor-bearing mice. These findings suggest that ^{64}Cu-NOTA-pertuzumab may be utilized for the sensitive detection of HER2-positive ovarian cancer.

Non-invasive imaging methods to evaluate HER2 expression status have been explored using monoclonal antibodies, antibody fragments, and affibodies [20–22]. Trastuzumab, an HER2-specific monoclonal antibody, is the most widely investigated platform for HER2-targeted imaging tracer [22]. In particular, preclinical studies of ^{89}Zr-labeled trastuzumab revealed high uptake in HER2-expressing cancers *in vivo* [23]. Pertuzumab is unique that it inhibits the dimerization process of HER2 with other HER family members, a mechanism that can obstruct tumor growth in combination with other chemotherapeutic drugs [10]. However, pertuzumab has not been well evaluated as a molecular imaging tracer. In 2009, McLarty *et al.* reported that ^{111}In-labeled pertuzumab can detect HER2 downregulation in a xenograft

model of breast cancer [24]. Recently, Marquez *et al.* evaluated ^{89}Zr-pertuzumab for imaging of HER2 in breast cancer xenografts, showing enhanced uptake (47.5 ± 32.9 %ID/g) in BT474 tumor xenografts [25]. In agreement with this study, we confirmed that radiolabeled pertuzumab allowed for the non-invasive imaging of HER2 expression in ovarian cancer models. Furthermore, this study revealed that radiolabeled pertuzumab could selectively and specifically target HER2 expression in both subcutaneous and orthotopic models of ovarian cancer.

ImmunoPET imaging is a relatively new field of study that relies on the innate specificity of antibodies towards their corresponding antigens. Molecular imaging of HER2 expression was first assessed over a decade ago using radiolabeled trastuzumab, yet the formation of intrinsic resistance mechanisms effectively limited the clinical translation of the tracer. Despite these pitfalls with trastuzumab, researchers have made significant progress in the development and characterization of antibody-based imaging tracers. There are several differences between pertuzumab and trastuzumab that may affect the potential clinical translation of these antibodies as imaging tracers. First, both antibodies show distinct binding properties to HER2, with trastuzumab and pertuzumab binding to domains IV and II of the extracellular HER2 receptor, respectively. Additionally, trastuzumab is a recombinant humanized IgG1 with a half-life of 25.5 days, while pertuzumab is a fully humanized IgG1κ with a much shorter half-life of only 10 days. Hence, the rapid clearance of radiolabeled pertuzumab from circulation may lead to improved tumor-to-blood ratios. Also, the mechanism of action greatly varies between the two antibodies [26], which may impact the overall tumor accumulation. Lastly, pertuzumab-based HER2 targeting agents may have a better chance for the clinical translation because of its lower immunogenecity and decreased chance of the tumor forming resistance to pertuzumab as compared to trastuzumab [26–28].

To ease the concern of radioactivity absorbed by patients, we utilized ^{64}Cu to label pertuzumab to minimize radiation dosage to patients. As expected, dosimetry data extrapolated to human subjects revealed a lower level of absorbed dose with ^{64}Cu-NOTA-pertuzumab when compared to ^{89}Zr, which is attributed to the short half-life of ^{64}Cu. Recently, Lam *et al.* developed ^{64}Cu-NOTA-Pertuzumab F(ab')$_2$ for monitoring changes if HER2 expression associated with trastuzumab therapy [29]. The radiolabeled antibody fragment resulted in lower predicted total body doses in humans by two-fold in comparison to the intact antibody (determined in this study) with values of 0.029 and 0.015 mSv/MBq for the intact and fragmented antibody, respectively. While ^{64}Cu limited the amount of time for longitudinal PET imaging, we obtained similar tumor uptake values when compared to ^{89}Zr-labeled pertuzumab in tumors with high HER2 expression. This rapid and enhanced uptake at an earlier time point is a distinct advantage for the successful clinical translation of a tracer.

Standard imaging methods for detection of peritoneal metastasis, such as CT and magnetic resonance imaging, are considerably limited with a per-lesion sensitivity of only 20% [30]. Diffusion-weighted magnetic resonance imaging (DW-MRI) shows higher sensitivity for small lesions, but the specificity may be limited by diffusion restriction [31]. Also, ^{18}F-fluorodeoxyglucose (^{18}F-FDG) PET/CT imaging is used to evaluate peritoneal metastasis in advanced ovarian cancer. However, nonspecific uptake of ^{18}F-FDG has been problematic in

ovarian cancer, effectively limiting the detection of small or diffusely infiltrative lesions [32]. The present study demonstrated that ^{64}Cu-NOTA-pertuzumab allows for clear delineation of small peritoneal implants (2 – 5 mm) in an orthotopic model of ovarian cancer. These findings support further evaluation of the tracer in patients with advanced ovarian cancer with peritoneal metastasis.

Conclusion

We investigated ^{64}Cu-labeled pertuzumab for PET imaging to evaluate HER2 expression noninvasively in ovarian cancer. ^{64}Cu-NOTA-pertuzumab displayed specific, rapid, and persistent accumulation in tumors with high HER2 expression (SKOV3), and the quantified uptake correlated well with HER2 expression levels. The enhanced targeting capability and high detection sensitivity of ^{64}Cu-NOTA-pertuzumab were further validated using orthotopic models, suggesting that the tracer could be employed for initial diagnosis and characterization of HER2-expressing malignancies, and for the sensitive detection of HER2-positive peritoneal metastases.

Supplementary Material

Refer to Web version on PubMed Central for supplementary material.

Acknowledgments

This work was supported, in part, by the University of Wisconsin - Madison, the National Institutes of Health (NIBIB/NCI 1R01CA169365, 1R01EB021336, P30CA014520, T32CA009206, T32GM008505, S10-OD018505), the American Cancer Society (125246-RSG-13-099-01-CCE), and the National Science Foundation of China (81401465, 51573096).

References

1. Berchuck A, Kamel A, Whitaker R, Kerns B, Olt G, Kinney R, et al. Overexpression of Her-2/Neu Is Associated with Poor Survival in Advanced Epithelial Ovarian-Cancer. Cancer Res. 1990; 50:4087–91. [PubMed: 1972347]
2. Bartlett JM, Langdon SP, Simpson BJ, Stewart M, Katsaros D, Sismondi P, et al. The prognostic value of epidermal growth factor receptor mRNA expression in primary ovarian cancer. Brit J Cancer. 1996; 73:301–6. DOI: 10.1038/bjc.1996.53 [PubMed: 8562334]
3. Tuefferd M, Couturier J, Penault-Llorca F, Vincent-Salomon A, Broet P, Guastalla JP, et al. HER2 status in ovarian carcinomas: a multicenter GINECO study of 320 patients. PLoS One. 2007; 2:e1138.doi: 10.1371/journal.pone.0001138 [PubMed: 17987122]
4. Magnifico A, Albano L, Campaner S, Delia D, Castiglioni F, Gasparini P, et al. Tumor-initiating cells of HER2-positive carcinoma cell lines express the highest oncoprotein levels and are sensitive to trastuzumab. Clin Cancer Res. 2009; 15:2010–21. DOI: 10.1158/1078-0432.CCR-08-1327 [PubMed: 19276287]
5. Arteaga CL, Sliwkowski MX, Osborne CK, Perez EA, Puglisi F, Gianni L. Treatment of HER2-positive breast cancer: current status and future perspectives. Nat Rev Clin Oncol. 2011; 9:16–32. DOI: 10.1038/nrclinonc.2011.177 [PubMed: 22124364]
6. Hodeib M, Serna-Gallegos T, Tewari KS. A review of HER2-targeted therapy in breast and ovarian cancer: lessons from antiquity - CLEOPATRA and PENELOPE. Future Oncol. 2015; 11:3113–31. DOI: 10.2217/fon.15.266 [PubMed: 26597460]
7. Solomayer EF, Becker S, Pergola-Becker G, Bachmann R, Kramer B, Vogel U, et al. Comparison of HER2 status between primary tumor and disseminated tumor cells in primary breast cancer patients. Breast Cancer Res Treat. 2006; 98:179–84. DOI: 10.1007/s10549-005-9147-y [PubMed: 16552629]

8. Seol H, Lee HJ, Choi Y, Lee HE, Kim YJ, Kim JH, et al. Intratumoral heterogeneity of HER2 gene amplification in breast cancer: its clinicopathological significance. Mod Pathol. 2012; 25:938–48. DOI: 10.1038/modpathol.2012.36 [PubMed: 22388760]
9. Baselga J, Cortes J, Kim SB, Im SA, Hegg R, Im YH, et al. Pertuzumab plus trastuzumab plus docetaxel for metastatic breast cancer. N Engl J Med. 2012; 366:109–19. DOI: 10.1056/NEJMoa1113216 [PubMed: 22149875]
10. Faratian D, Zweemer AJ, Nagumo Y, Sims AH, Muir M, Dodds M, et al. Trastuzumab and pertuzumab produce changes in morphology and estrogen receptor signaling in ovarian cancer xenografts revealing new treatment strategies. Clin Cancer Res. 2011; 17:4451–61. DOI: 10.1158/1078-0432.CCR-10-2461 [PubMed: 21571868]
11. Scheuer W, Friess T, Burtscher H, Bossenmaier B, Endl J, Hasmann M. Strongly enhanced antitumor activity of trastuzumab and pertuzumab combination treatment on HER2-positive human xenograft tumor models. Cancer Res. 2009; 69:9330–6. DOI: 10.1158/0008-5472.CAN-08-4597 [PubMed: 19934333]
12. Lua W-H, Gan SK-E, Lane DP, Verma CS. A search for synergy in the binding kinetics of Trastuzumab and Pertuzumab whole and F(ab) to Her2. npj Breast Cancer. 2015; 1:15012.doi: 10.1038/npjbcancer.2015.12
13. Siegel RL, Miller KD, Jemal A. Cancer statistics, 2016. CA Cancer J Clin. 2016; 66:7–30. DOI: 10.3322/caac.21332 [PubMed: 26742998]
14. Luo H, Hernandez R, Hong H, Graves SA, Yang Y, England CG, et al. Noninvasive brain cancer imaging with a bispecific antibody fragment, generated via click chemistry. Proc Natl Acad Sci U S A. 2015; 112:12806–11. DOI: 10.1073/pnas.1509667112 [PubMed: 26417085]
15. Yang Y, Hernandez R, Rao J, Yin L, Qu Y, Wu J, et al. Targeting CD146 with a ^{64}Cu-labeled antibody enables *in vivo* immunoPET imaging of high-grade gliomas. Proc Natl Acad Sci U S A. 2015; 112:E6525–34. DOI: 10.1073/pnas.1502648112 [PubMed: 26553993]
16. Stabin MG. MIRDOSE: personal computer software for internal dose assessment in nuclear medicine. J Nucl Med. 1996; 37:538–46. [PubMed: 8772664]
17. Protection R. ICRP publication 103. Ann ICRP. 2007; 37:2.
18. England CG, Ehlerding EB, Hernandez R, Rekoske BT, Graves SA, Sun H, et al. Preclinical Pharmacokinetics and Biodistribution Studies of ^{89}Zr-labeled Pembrolizumab. J Nucl Med. 2016; doi: 10.2967/jnumed.116.177857
19. Bhattacharyya S, Kurdziel K, Wei L, Riffle L, Kaur G, Hill GC, et al. Zirconium-89 labeled panitumumab: a potential immuno-PET probe for HER1-expressing carcinomas. Nucl Med Biol. 2013; 40:451–7. DOI: 10.1016/j.nucmedbio.2013.01.007 [PubMed: 23454247]
20. Tang Y, Wang J, Scollard DA, Mondal H, Holloway C, Kahn HJ, et al. Imaging of HER2/neu-positive BT-474 human breast cancer xenografts in athymic mice using (111)In-trastuzumab (Herceptin) Fab fragments. Nucl Med Biol. 2005; 32:51–8. DOI: 10.1016/j.nucmedbio.2004.08.003 [PubMed: 15691661]
21. Kramer-Marek G, Kiesewetter DO, Capala J. Changes in HER2 expression in breast cancer xenografts after therapy can be quantified using PET and (18)F-labeled affibody molecules. J Nucl Med. 2009; 50:1131–9. DOI: 10.2967/jnumed.108.057695 [PubMed: 19525458]
22. Perik PJ, Lub-De Hooge MN, Gietema JA, van der Graaf WT, de Korte MA, Jonkman S, et al. Indium-111-labeled trastuzumab scintigraphy in patients with human epidermal growth factor receptor 2-positive metastatic breast cancer. J Clin Oncol. 2006; 24:2276–82. DOI: 10.1200/JCO.2005.03.8448 [PubMed: 16710024]
23. Dijkers EC, Kosterink JG, Rademaker AP, Perk LR, van Dongen GA, Bart J, et al. Development and characterization of clinical-grade ^{89}Zr-trastuzumab for HER2/neu immunoPET imaging. J Nucl Med. 2009; 50:974–81. DOI: 10.2967/jnumed.108.060392 [PubMed: 19443585]
24. McLarty K, Cornelissen B, Cai Z, Scollard DA, Costantini DL, Done SJ, et al. Micro-SPECT/CT with 111In-DTPA-pertuzumab sensitively detects trastuzumab-mediated HER2 downregulation and tumor response in athymic mice bearing MDA-MB-361 human breast cancer xenografts. J Nucl Med. 2009; 50:1340–8. DOI: 10.2967/jnumed.109.062224 [PubMed: 19617342]

25. Marquez BV, Ikotun OF, Zheleznyak A, Wright B, Hari-Raj A, Pierce RA, et al. Evaluation of (89)Zr-pertuzumab in Breast cancer xenografts. Mol Pharm. 2014; 11:3988–95. DOI: 10.1021/mp500323d [PubMed: 25058168]

26. Capelan M, Pugliano L, De Azambuja E, Bozovic I, Saini KS, Sotiriou C, et al. Pertuzumab: new hope for patients with HER2-positive breast cancer. Ann Oncol. 2013; 24:273–82. DOI: 10.1093/annonc/mds328 [PubMed: 22910839]

27. Reynolds K, Sarangi S, Bardia A, Dizon DS. Precision medicine and personalized breast cancer: combination pertuzumab therapy. Pharmgenomics Pers Med. 2014; 7:95–105. DOI: 10.2147/PGPM.S37100 [PubMed: 24715764]

28. Jackisch C, Kim SB, Semiglazov V, Melichar B, Pivot X, Hillenbach C, et al. Subcutaneous versus intravenous formulation of trastuzumab for HER2-positive early breast cancer: updated results from the phase III HannaH study. Ann Oncol. 2015; 26:320–5. DOI: 10.1093/annonc/mdu524 [PubMed: 25403587]

29. Lam K, Chan C, Reilly RM. Development and preclinical studies of ^{64}Cu-NOTA-pertuzumab F(ab')2 for imaging changes in tumor HER2 expression associated with response to trastuzumab by PET/CT. MAbs. 2017; 9:154–64. DOI: 10.1080/19420862.2016.1255389 [PubMed: 27813707]

30. Kyriazi S, Kaye SB, deSouza NM. Imaging ovarian cancer and peritoneal metastases–current and emerging techniques. Nat Rev Clin Oncol. 2010; 7:381–93. DOI: 10.1038/nrclinonc.2010.47 [PubMed: 20386556]

31. Dhanda S, Thakur M, Kerkar R, Jagmohan P. Diffusion-weighted imaging of gynecologic tumors: diagnostic pearls and potential pitfalls. Radiographics. 2014; 34:1393–416. DOI: 10.1148/rg.345130131 [PubMed: 25208287]

32. Sironi S, Messa C, Mangili G, Zangheri B, Aletti G, Garavaglia E, et al. Integrated FDG PET/CT in patients with persistent ovarian cancer: correlation with histologic findings. Radiology. 2004; 233:433–40. DOI: 10.1148/radiol.2332031800 [PubMed: 15516617]

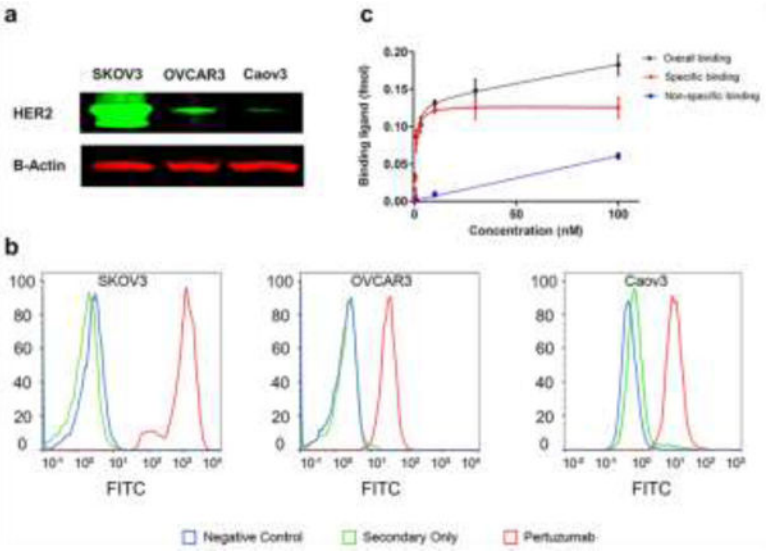

Fig. 1.

Evaluation of binding affinity of pertuzumab to HER2. (A) Western blot analysis of HER2 expression in three ovarian cancer cell lines showed high expression in SKOV3 cells and low expression in OVCAR3 and Caov3 cells. (B) HER2 expression was examined using flow cytometry, revealing high HER2 expression of SKOV3 cells and low levels of HER2 expression by OVCAR3 and Caov3 cells. (C) Saturation binding assays showed that ^{64}Cu-NOTA-pertuzumab displayed specific binding to SKOV3 cells, with a receptor density of 1.6 million HER2 receptors per SKOV3 cell.

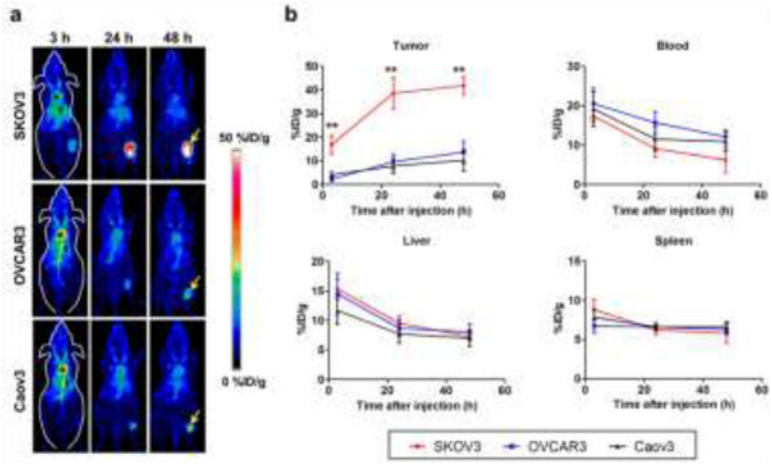

Fig. 2.

PET imaging and quantitative analysis of HER2 expression with ^{64}Cu-NOTA-pertuzumab in subcutaneous ovarian cancer models. (A) PET maximum intensity projection (MIP) images at 3, 24, and 48 h after injection of ^{64}Cu-NOTA-pertuzumab. Arrow: tumor, *: blood pool, †: liver (B) Time-activity curves of region-of-interest (tumor, blood, liver, and spleen) after intravenous injection of ^{64}Cu-NOTA-pertuzumab in three subcutaneous ovarian cancer models. ^{64}Cu-NOTA-pertuzumab kinetics in the blood pool, liver, and spleen showed no significant difference between the three groups. **: $P < 0.01$

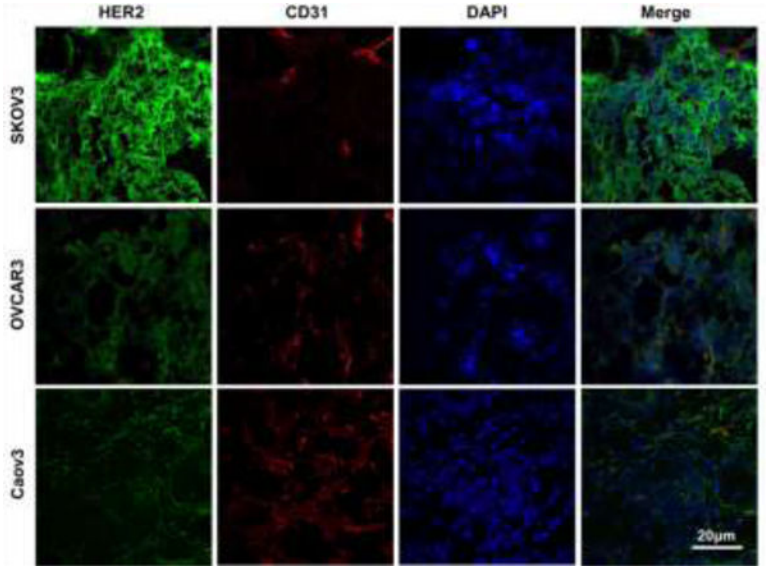

Fig. 3.

Immunofluorescence staining of tumor tissue sections. Pertuzumab and FITC-labeled anti-human secondary antibody were used for HER2 staining (green), CD31 was stained to expose locations of the vasculature (red), and DAPI was used for the visualization of cell nuclei locations (blue). Scale bar = 20 μm

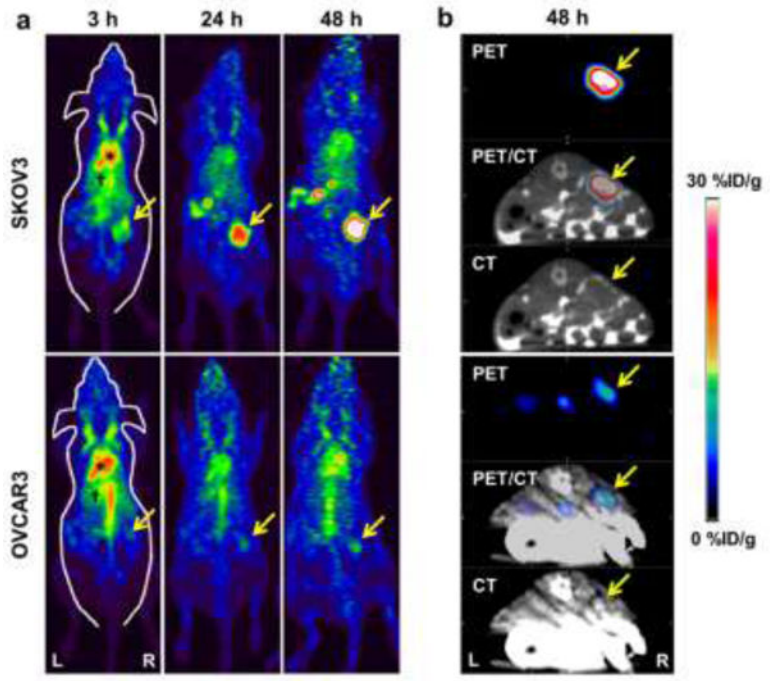

Fig. 4.

PET/CT imaging of HER2 expression in orthotopic models of ovarian cancer. (A) PET maximum intensity projection (MIP) images at 3, 24, and 48 h after injection of ^{64}Cu-NOTA-pertuzumab in SKOV3 and OVCAR3 orthotopic ovarian models, where tumors are indicated by arrows. (B) Representative transverse PET/CT images of SKOV3 and OVCAR3 tumor-bearing mice at 48 h after injection of ^{64}Cu-NOTA-pertuzumab (n = 4, for each group).

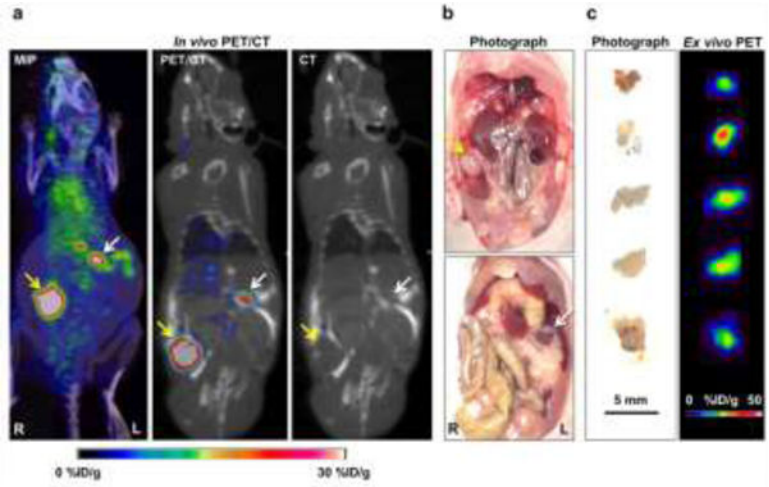

Fig. 5.

Radiological-surgical correlation of SKOV3 orthotopic ovarian cancer model. (A) In PET/CT imaging, a primary tumor with strong uptake was found in the right ovary area (yellow arrow), and there were many focal uptakes in the peritoneal space (white arrow). (B) Surgical exploration was done in the same animal after terminal PET/CT imaging. The primary tumor mass was found in the right ovary (yellow arrow), and there was white nodular tissue (white arrow) at the location of focal uptake on the PET/CT imaging, suggesting peritoneal implants. (C) *Ex vivo* PET imaging of excised peritoneal implants was performed. The small peritoneal implants showed high PET uptake values.

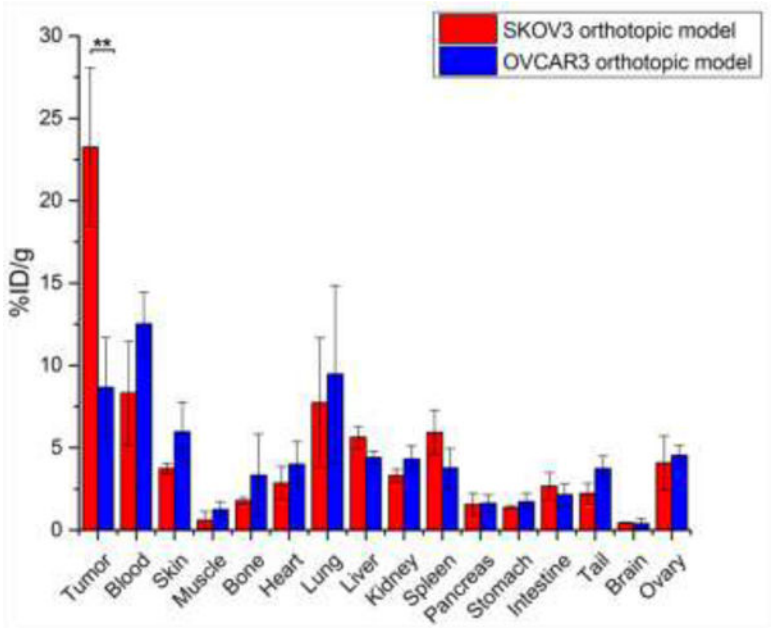

Fig. 6. Ex vivo

biodistribution studies for the validation of PET/CT results. Biodistribution of ^{64}Cu-NOTA-pertuzumab in SKOV3 and OVCAR3 orthotopic ovarian cancer models at 48 h after injection (n = 4). SKOV3 tumors showed a significantly higher tracer accumulation comparing to OVCAR3 tumors, while normal ovaries in both groups displayed the low levels of ^{64}Cu-NOTA-pertuzumab uptake.